

# Reaction Dynamics for Fusion of Weakly-Bound Nuclei

Kouichi HAGINO<sup>1</sup> and Andrea VITTURI<sup>2</sup>

<sup>1</sup>*Yukawa Institute for Theoretical Physics, Kyoto University,  
Kyoto 606-8502, Japan*

<sup>2</sup>*Dipartimento di Fisica, Universita di Padova and INFN, I-35131 Padova, Italy*

We discuss several open problems of fusion reactions induced by weakly bound nuclei. For this purpose, we solve a one dimensional three-body Hamiltonian with the coupled-channels formalism. We show that the continuum-continuum couplings substantially reduce the total fusion probability at energies above the barrier compared with the no-breakup case, although the fusion probability remains enhanced at subbarrier energies. We then discuss a role of transfer process in fusion of weakly bound nuclei, and point out that removing spurious Pauli forbidden transfer components from the calculation may be crucial at energies below the barrier. Calculations based on the three-body classical trajectory Monte Carlo (CTMC) method are also presented in order to discuss how to model complete fusion process.

## §1. Introduction

The recent availability of radioactive beams has opened up the opportunity to study the interactions and structure of exotic nuclei close to the drip lines. Unstable neutron-rich nuclei having very weakly bound neutrons exhibit characteristic features such as a neutron halo and a low energy threshold for breakup. These features may dramatically affect fusion and other reaction processes.

One of the main issues in the study of reaction induced by weakly-bound nuclei is to clarify how the breakup process influences fusion reactions at energies close to the Coulomb barrier.<sup>1)–10)</sup> In Ref. 4), we have performed coupled-channels calculations in order to address this question by discretizing in energy the particle continuum states of the projectile nucleus. Defining the complete fusion as absorption from bound state channels, we have demonstrated that fusion cross sections are determined by the competition of two mechanisms, i.e. dynamical modulation of fusion barrier and flux loss due to the breakup couplings. Their net effect differs depending on the bombarding energy: the *complete* fusion cross sections are enhanced at energies below the barrier, while they are hindered above the barrier, compared with cross sections for a tightly bound system. On the other hand, the *total* fusion cross sections (a sum of complete and incomplete fusion cross sections) are enhanced at subbarrier energies while they are close to the no-breakup calculations at above. In these calculations, we did not include the couplings among the continuum channels.

In this contribution, we would like to discuss how these conclusions may be altered by more refined calculations. We particularly pay attention to the definition of complete fusion, the role of continuum-continuum couplings, and the effect of transfer channels. To this end, we solve a simple one dimensional three-body Hamiltonian with the coupled-channels method. As we will show below, our main conclusions for the complete fusion remain valid at least in a qualitative way, although we find that the total fusion cross sections are hindered at energies above the barrier due to the

continuum-continuum couplings.

## §2. Separation of complete and incomplete fusion

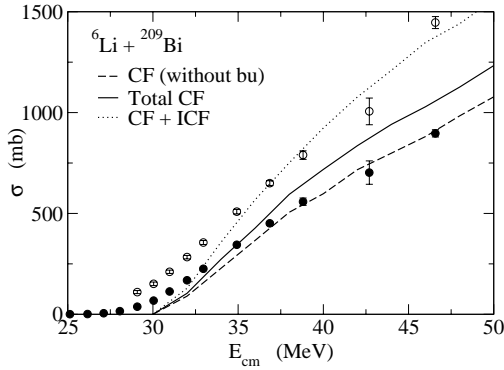


Fig. 1. Comparison of the three-body classical trajectory Monte Carlo calculations with the experimental data for  ${}^6\text{Li} + {}^{209}\text{Bi}$  reaction. The solid and the dotted lines are complete and total fusion cross sections, respectively. The contribution of the absorption of the whole projectile from bound states is denoted separately by the dashed line. The experimental data are taken from Ref. 8).

cross sections.

In order to estimate the contribution of the breakup followed by complete fusion, one of us has developed a three body classical trajectory Monte Carlo (CTMC) method.<sup>8)</sup> For a three body Hamiltonian that consists of the target ( $T$ ) and two projectile fragments ( $P_1$  and  $P_2$ ), two-dimensional classical Newtonian equations are solved to obtain the time evolution of the coordinates and velocities of the fragments. The initial conditions are that the projectile, with its two fragments in random orientation, starts far from the target with impact parameter  $b$ . As the projectile moves towards the target, three processes are possible, depending the value of the impact parameter  $b$ : (i) the projectile as a whole or both of the fragments are absorbed by the target, (ii) only one fragment is absorbed, and (iii) neither fragment is captured. We assume that the breakup occurs when the distance between the projectile fragments exceeds their potential barrier radius, and that the projectile fragment  $P_i$  is absorbed by the target nucleus when the relative distance between the target and the fragment is smaller than  $r_{\text{abs}} = 1.1 \times (A_T^{1/3} + A_{P_i}^{1/3})$ . See also Ref. 11) for details.

Figure 1 shows the results of the three body CTMC method for the fusion reaction of  ${}^6\text{Li} + {}^{209}\text{Bi}$ .<sup>8)</sup> The dotted line denotes the sum of complete and incomplete

Theoretically, the complete fusion refers to the capture of the whole projectile, while the incomplete fusion is a process where only a part of the projectile is captured. In our previous calculations,<sup>4)</sup> we defined complete fusion as absorption from bound state channels, while the incomplete fusion as those from continuum state channels in the projectile. The basic idea was that a continuum state is a doorway of breakup, and thus is related to incomplete fusion process. However, when the breakup takes place inside the Coulomb barrier, all the breakup fragments would likely be captured by the target nucleus, leading to complete fusion reaction.<sup>8), 9)</sup> This breakup followed by complete fusion was not taken into account in the definition of complete fusion in Ref. 4), and the previous calculation provides only the lower limit of complete fusion

fusion cross sections. Since this is a classical calculation, cross sections are finite only at energies above the Coulomb barrier. The dashed line indicates the absorption of the whole projectile from the bound states, while the solid line shows the total complete fusion cross sections. The difference between the solid and the dashed line thus represents the contribution from the breakup followed by the complete fusion process. As we see, there is a significant contribution of this process at energies above the barrier. This process has not been considered in any coupled-channels calculations so far, and the present result suggests that a consistent definition of complete fusion is necessary when one compares experimental data with theoretical calculations.

### §3. Role of continuum-continuum couplings

Let us now discuss the effect of continuum-continuum couplings in the coupled-channels calculations. Diaz-Torres and Thompson showed that this effect increases the irreversibility of breakup process, and thus hinders the total fusion cross sections.<sup>5)</sup> In fact, their calculation suggests that the total fusion cross sections are smaller than the no-coupling case at energies above the barrier, although those are larger at energies below the barrier. A similar hindrance has been found in the time dependent wave packet approach of Yabana et al.<sup>6), 7)</sup> Their calculations indicate that the total fusion probability is smaller than that for the core-target system, suggesting that it is much smaller than the prediction of the folding model calculation, which statically takes into account the halo structure of the projectile nucleus. They attribute this hindrance of fusion probability to a spectator role of the valence neutron.<sup>6), 7)</sup> In this section, we revisit this problem and discuss whether the hindrance of total fusion probability observed in the time dependent wave packet approach can be understood in terms of the effect of continuum-continuum couplings in the coupled-channels approach.

To this end, we use a one dimensional three-body Hamiltonian which was used by Yabana and Suzuki for their time-dependent wave packet calculation for fusion of  $^{10}\text{Li} + ^{40}\text{Ca}$  system.<sup>6)</sup> Assuming that the projectile consists of a core nucleus ( $C$ ) and a valence neutron ( $n$ ), and that the target mass is infinite, the model Hamiltonian reads<sup>6)</sup>

$$H = -\frac{\hbar^2}{2M} \frac{\partial^2}{\partial X^2} + V_{CT} \left( X - \frac{m_n}{M} x \right) + V_{nT} \left( X + \frac{m_C}{M} x \right) - \frac{\hbar^2}{2\mu} \frac{\partial^2}{\partial x^2} + V_{nC}(x), \quad (3.1)$$

where  $X$  and  $x$  are the relative coordinate between the target and the center of mass of the projectile, and that between the core and the valence neutron in the projectile, respectively.  $M = m_n + m_C$  is the total mass of the projectile, while  $\mu = m_n \cdot m_C / M$  is the reduced mass for core-neutron system. We use the same potentials with the same values for the parameters as in Ref. 6), except for the  $X_M$  parameter in the Coulomb interaction which we somewhat increase in order to increase the barrier height.

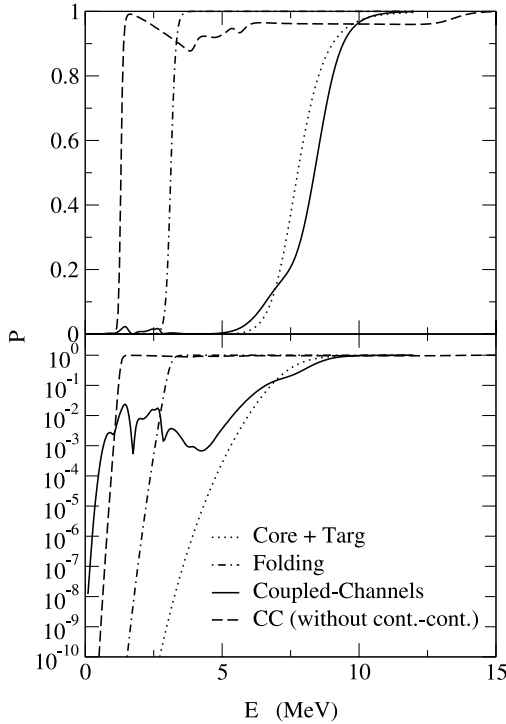


Fig. 2. The total penetrability for the one dimensional three body Hamiltonian obtained by the several methods. The solid and the dashed lines are the results of the coupled-channels calculations with and without the continuum-continuum couplings, respectively. The dot-dashed line is the penetrability for the folding potential, while the dotted line denotes the penetrability for the core-target system.

linear (the upper panel) and in the logarithmic scale (the lower panel). We include the first seven discretized continuum states together with the ground state. At low energies, some of the continuum states are kinematically forbidden (i.e. closed channels), and it is not easy to obtain numerically stable solutions of the coupled-channels equations. We avoid this problem by using the modified log-derivative method.<sup>13)</sup> This method is in fact very powerful, and we have confirmed that our results are stable against the mesh size and the matching radius. We have also checked that the low energy penetrability does not change much even when we include more continuum state channels in the coupled-channels equations. The penetrability still shows a resonance-like structure. This occurs at a threshold energy for each discretized channel, and can thus be attributed to the threshold effect.<sup>14)</sup>

The result of the coupled-channels calculations is compared with the fusion prob-

In order to solve this Hamiltonian with the coupled-channels framework, we first obtain the eigenstates for the projectile Hamiltonian,  $H_{\text{proj}} = -\frac{\hbar^2}{2\mu} \frac{d^2}{dx^2} + V_n C(x)$ , by expanding the wave functions on the orthogonal polynomial basis, which was recently advocated by Pérez-Bernal et al.<sup>12)</sup> This basis is constructed from the ground state wave function of the Hamiltonian  $\phi_0(x)$  by multiplying a polynomial function to it ( $\phi_0, x\phi_0, x^2\phi_0, \dots, x^n\phi_0$ ). Since the wave function is expanded on the discrete basis, the continuum states, obtained by diagonalizing the Hamiltonian, are also discretized in energy. We use the polynomial basis up to  $n = 28$ . The energy for the first five states is given by:  $\epsilon_0 = -26.09$  MeV,  $\epsilon_1 = -11.42$  MeV,  $\epsilon_2 = -0.515$  MeV,  $\epsilon_3 = 0.135$  MeV, and  $\epsilon_4 = 0.193$  MeV. Following Ref. 6), we assume that the ground and the first excited states in this Hamiltonian are occupied by the neutrons in the core nucleus, and consider the second excited state as the ground state of the core-neutron system,  $\phi_{gs}(x)$ .

Figure 2 shows the total barrier penetrability obtained with the coupled-channels method (the solid line) in the

ability (barrier penetrability) for the folding potential (the dot-dashed line),

$$V_{\text{fold}}(X) = \int dx \phi_{gs}(x)^2 \left[ V_{CT} \left( X - \frac{m_n}{M} x \right) + V_{nT} \left( X + \frac{m_C}{M} x \right) \right]. \quad (3.2)$$

We find that the total penetrability is significantly hindered by the continuum couplings at energies above the barrier height of the folding potential, although it is still enhanced compared with the penetrability for the folding potential at energies below the barrier (see the lower panel). Notice that the total penetrability is even smaller than the penetrability for the core-target system (the dotted line) at energies above the barrier. This is reminiscent of the result of the time dependent wave packet approach.<sup>6)</sup>

The result without the continuum-continuum couplings is denoted by the dashed line. As was pointed out in Ref. 5), this calculation significantly overestimates the barrier penetrability compared with the full coupled-channels calculation. A part of the reason why the continuum-continuum couplings reduce the penetrability can be understood as follows: the wave function of the (discretized) continuum state considerably extends outside the barrier. The diagonal matrix element of the coupling Hamiltonian for a continuum state channel is thus much smaller than that for the ground state, Eq. (3.2). Notice that the diagonal matrix element is given by the folding potential itself for all the channels if the continuum-continuum couplings are neglected. The change of the diagonal matrix elements can be regarded as “effective  $Q$ -value”, which is large and positive around the barrier region. If the coupling is strong enough, the penetrability can then be reduced due to the so called anti-adiabatic effect.<sup>15), 16)</sup>

#### §4. Role of transfer process

We next discuss the effect of transfer couplings on fusion of a halo nucleus. Compared with the breakup effects, a discussion on the transfer effect has yet been scarce.<sup>16)</sup> The time dependent wave packet approach of Yabana et al. shows that the fusion probability is hindered over that for the core-target system even at energies well below the barrier.<sup>7)</sup> This conclusion is qualitatively different from the result of the coupled-channels approach,<sup>4), 5)</sup> which predicts an enhancement of fusion probability at low energies, as was discussed in the previous section. In both of these approaches, the multipole decomposition is usually introduced to the total wave function. Yabana et al. examined the effect of the angular momentum truncation for the neutron-core system, and showed that the fusion probability is enhanced when the angular momentum is limited to low values.<sup>7)</sup> A high value for the angular momentum is required in order to simulate the transfer process of the neutron to the target nucleus, and Yabana et al. claimed that the enhancement of fusion cross sections found in the coupled-channels approach is an artifact of neglecting the transfer coupling. They needed up to  $l = 70$  in order to get a converged result. Diaz-Torres and Thompson also studied the effect of angular momentum truncation in the coupled-channels framework.<sup>5)</sup> Their result seems to indicate that the fusion cross sections indeed get smaller when higher angular momentum components are

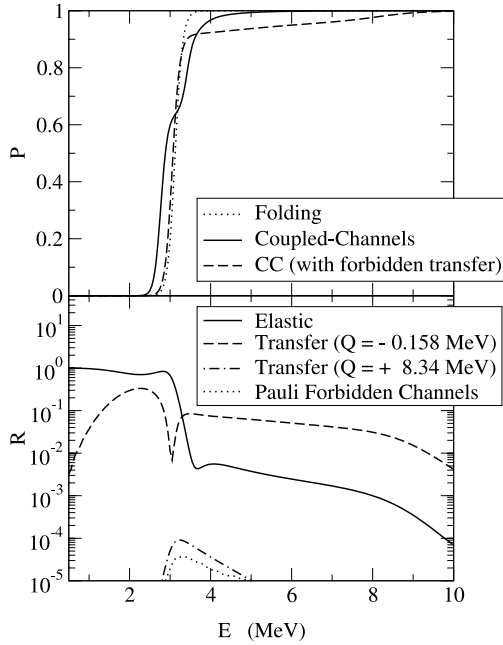


Fig. 3. The effect of the Pauli forbidden transfer channels on the transmission (the upper panel) and the reflection (the lower panel) probabilities. The dashed and the solid lines in the upper panel are obtained by solving the coupled-channels equations with and without the Pauli forbidden channels, respectively. The dotted line in the upper panel is the penetrability for the folding potential. The solid line in the lower panel is the reflection probability for the incident channel obtained by the coupled-channels calculation with the Pauli forbidden channels. The dashed and the dot-dashed lines are the transfer probabilities for the highest and the second highest bound states in the target nucleus. The total reflection probability for the Pauli forbidden channels is denoted by the dotted line.

specified in the previous section, there are five bound states in the target nucleus at  $-40.5$ ,  $-31.9$ ,  $-20.6$ ,  $-8.85$  and  $-0.357$  MeV. We assume that the ground state as well as the first and the second excited states in this Hamiltonian are already occupied. The solid line in the upper panel of Fig. 3 is the result of the coupled-channels calculation where only the transfer channels to the two allowed states in the target are included. We compute the transfer coupling matrix elements in the no-recoil approximation using the neutron-target potential  $V_{nT}$  as the transfer interaction. In order to mimic the recoil effect, we multiply a factor of  $2(m_C + 1)/(2m_C + 1)$

included in the calculation (see Fig. 6 in Ref. 5)).

However, we here ask a general question: is it really physical to include all the partial wave components for the neutron-core system? It is true that one can in principle solve the three-body Hamiltonian exactly if one includes all the partial waves. In such a calculation, *all* the transfer channels are automatically entered. Notice that these include even a transfer to a deep bound state of the target nucleus, which must be forbidden by the Pauli principle. Those Pauli forbidden transfer channels most likely have a large positive  $Q$ -value, and the fusion cross sections may be artificially hindered due to the anti-adiabatic effect<sup>15)</sup> if these channels are included in the calculation. Also, when the initial configuration of the valence neutron is at an excited state of the Hamiltonian due to the Pauli principle, the forbidden de-excitations to lower states in the projectile may be entered unless those transitions are explicitly excluded by e.g. the basis expansion. Those forbidden de-excitations may also lead to an artificial reduction of fusion cross sections for the same reason.

In order to examine the effect of the spurious Pauli forbidden transfer channels in the projectile, we again solve the one dimensional three body model in the previous section with the coupled-channels method by including several transfer channels. For the parameter set

to the transfer matrix elements.<sup>17),18)</sup> For simplicity, the continuum excited states in the projectile are not included. In this calculation, one can clearly see that the fusion probability is enhanced due to the transfer couplings at energies below the barrier compared with the folding model calculation (the dotted line). The result of the coupled-channels calculation with the Pauli forbidden channels is given by the dashed line. One sees that the enhancement of fusion probability is much less at energies below the barrier due to the anti-adiabatic effect.

The lower panel of Fig. 3 shows the reflection probabilities for the elastic (the solid line) and the transfer channels. The dashed and the dot-dashed lines represent the transfer probability for the highest and the second highest bound states in the target nucleus, respectively. Due to the  $Q$ -value matching, the total transfer probability is dominated by the former, as has been found in the time dependent wave packet approach.<sup>6)</sup> The dotted line is the total reflection probability for the Pauli forbidden channels. Notice that this probability is much smaller than the transfer probability for the allowed channels, and may be negligible compared to the latter. Yet, the Pauli forbidden processes influence the barrier penetrability (the fusion probability) in a significant way. We thus conclude that care must be taken in discussing the angular momentum truncation, especially at energies around the barrier.

## §5. Summary and discussion

Two alternative approaches have been used in the literature in order to discuss the subbarrier fusion reaction induced by a weakly bound nuclei. A traditional approach is to solve the coupled-channels equations by discretizing in energy the continuum states in the projectile nucleus (CDCC). The second approach employs the time dependent dynamics and solves the time evolution of a wave packet. If one neglects the dynamical effects, the total fusion probabilities would have been larger than that for the core-target system, since the barrier height is considerably reduced due to a large extension of neutron wave function in the projectile nucleus. On the contrary, the time dependent approach predicts smaller fusion probabilities, suggesting that there is a huge dynamical effect which compensates the static effect. Using a simple one dimensional three body Hamiltonian, we have demonstrated that this result can be understood in terms of the effect of couplings among the continuum states. In this conference, Signorini et al. reported that the measured fusion cross sections for the  $^{11}\text{Be}+^{209}\text{Bi}$  are similar to those for the  $^{10}\text{Be}+^{209}\text{Bi}$  system despite the halo structure of the  $^{11}\text{Be}$  nucleus.<sup>10)</sup> It might be that the enhancement of fusion cross sections due to the static effect (reduction of the barrier height due to the halo structure) is compensated by the dynamical breakup effect, resulting in similar cross sections between the two systems.

At energies below the barrier, the two theoretical approaches predict a contradictory result to each other. In the coupled-channels approach, the fusion probability is found to be larger than the prediction of the folding model. In contrast, the time dependent wave packet approach predicts a hindrance of fusion probability even at energies below the barrier. We have argued that care must be taken in the partial

wave decomposition for the wave functions because spurious Pauli forbidden transfer channels are inevitably coupled when all the partial waves are included. We have found that the Pauli forbidden transfer couplings significantly hinder the total fusion probability even if the transfer probability itself may be negligible.

In order to draw a more definite conclusion on fusion cross sections for a weakly bound system at energies below the barrier, further calculations would be required by including only the Pauli allowed transfer channels together with the breakup channels. The time dependent wave packet approach would need to introduce the projection operator in order to exclude explicitly the Pauli forbidden channels. In the coupled-channels approach, the angular momentum between the core and the valence neutron should be limited to low values in order to avoid the Pauli forbidden transfer, and should explicitly include the transfer couplings in addition to the breakup channels. The combined effect of breakup and transfer in the coupled-channels approach has not been studied so far in the context of subbarrier fusion, and it would be an interesting future work.

A further complication arises from a separation of complete and incomplete fusion cross sections. Using the three body classical trajectory Monte Carlo method, we have demonstrated that there is a significant contribution of the breakup followed by complete fusion process to the total complete fusion cross sections. It would be another interesting future problem to model this process using a quantum mechanical model for subbarrier fusion of unstable nuclei.

### References

- 1) M. S. Hussein, M. P. Pato, L. F. Canto and R. Donangelo, *Phys. Rev. C* **46** (1992), 377.  
W. H. Z. Cardenas, L. F. Canto, R. Donangelo, M. S. Hussein, J. Lubian and A. Romanelli, *Nucl. Phys. A* **703** (2002), 633.
- 2) N. Takigawa, M. Kuratani and H. Sagawa, *Phys. Rev. C* **47** (1993), R2470.
- 3) C. H. Dasso and A. Vitturi, *Phys. Rev. C* **50** (1994), R12.
- 4) K. Hagino, A. Vitturi, C. H. Dasso, and S. M. Lenzi, *Phys. Rev. C* **61** (2000), 037602.
- 5) A. Diaz-Torres and I. J. Thompson, *Phys. Rev. C* **65** (2002), 024606.
- 6) K. Yabana and Y. Suzuki, *Nucl. Phys. A* **588** (1995), 99c.  
K. Yabana, *Prog. Theor. Phys.* **97** (1997), 437.
- 7) K. Yabana, M. Ueda and T. Nakatsukasa, *A* **722** (2003), 261c.
- 8) M. Dasgupta et al., *Phys. Rev. Lett.* **82** (1999), 1395; *Phys. Rev. C* **66** (2002), 041602(R).
- 9) I. Padron et al., *Phys. Rev. C* **66** (2002), 044608.
- 10) C. Signorini et al., *Eur. Phys. J. A* **2** (1998), 227, and contribution to *Prog. Theor. Phys. Suppl. No. 154* (2004), 272.
- 11) K. Hagino, M. Dasgupta, and D. J. Hinde, *Nucl. Phys. A* (to be published).
- 12) F. Pérez-Bernal, I. Martel, J. M. Arias and J. Gómez-Camacho, *Phys. Rev. A* **67** (2003), 052108.
- 13) W. Brenig and R. Russ, *Surf. Sci.* **315** (1994), 195.  
W. Brenig, T. Brunner, A. Gross and R. Russ, *Z. Phys. B* **93** (1993), 91.
- 14) K. Hagino and A. B. Balantekin, (to be published).
- 15) N. Rowley, I. J. Thompson and M. A. Nagarajan, *Phys. Lett. B* **282** (1992), 276.
- 16) W. von Oertzen and I. Krouglov, *Phys. Rev. C* **53** (1996), R1061.
- 17) H. Esbensen, S. H. Fricke and S. Landowne, *Phys. Rev. C* **40** (1989), 2046.
- 18) J. M. Quesada, G. Pollarolo, R. A. Broglia and A. Winther, *Nucl. Phys. A* **442** (1985), 381.